3D-QSAR Study on Diindolylmethane and Its Analogues with Comparative Molecular Field Analysis (CoMFA)

BENABADJI, Sakina Hayat[a]　　　CHEN, Hai-Feng[b](陈海峰)　　　YUAN, Shen-Gang[*,b](袁身刚)
WEN, Ren[*,a](闻韧)

[a] *Department of Medicinal Chemistry, Medical Center of Fudan University, Shanghai 200032, China*

[b] *Key Laboratory of Computer Chemistry, Shanghai Institute of Organic Chemistry, Chinese Academy of Sciences, Shanghai 200032, China*

Comparative molecular field analysis (CoMFA), a three dimensional quantitative structure-activity relationship (3D-QSAR) method was applied to a series of diindolylmethane (DIM) analogs to study the relationship between their structure and their induction of CYP 1A1-associated ethoxyresorufin-O-deethylase (EROD) activity. A DISCO model of pharmacophore was derived to guide the superposition of the compounds. The coefficient of cross-validation (q^2) and non cross-validation (r^2) for the model established by the study are 0.827 and 0.988 respectively, the value of variance ratio (F) is 103.53 and standard error estimate (SEE) is 0.044. These values indicate that the CoMFA model derived is significant and might have a good prediction for the catalytic activity of DIM compounds. As a consequence, the predicted activity values of new designed compounds were all higher than that of the reported value.

Keywords　　3D-QSAR, CoMFA, diindolylmethane, CYP 1A1

Introduction

Breast cancer is one of the leading causes of premature death in North American women. It is an estrogen-dependent cancer,[1] where various antiestrogen have been extensively developed for its treatment, such as benzothiophene, progesterone, and the current tamoxifen, which primarily act by blocking estrogen receptor (ER) action.[2] In the last several years, great attention has been devoted to diindolylmethane (DIM). 3,3-Diindolylmethane is an acid-catalyzed condensation product of indole-3-carbinol, a natural component of *Brassica* vegetables, and is formed in the stomach.[3] The antitumor properties of indole-3-carbinol for estrogen-dependent breast cancers are related, in part, to its ability to alter estrogen metabolism *in vitro* and *in vivo*.[4] Indole-3-carbinol is only active orally and rapidly oligomerizes in the stomach. Thus, the anticarcinogenic properties have been attributed to some of its condensation products, including the dimer DIM and indolocarbazole (ICZ). In contrast to ICZ, in rats, DIM

is a weak agonist for the aryl hydrocarbon receptor (AhR), also called the TCDD (2,3,7,8-tetrachlorodibenzo-*p*-dioxin) receptor, and induces hepatic cytochrome P450 (CYP) 1A1, 1A2, and their associated catalytic activity of ethoxyresorufin-O-deethylase (EROD).[5]

Recently, the antiestrogenic and antitumorigenic activities of the DIM derivatives are being investigated. Indeed, methyl-substituted DIM was demonstrated to be selective AhR modulators with potential for clinical treatment of breast cancer,[6] and symmetrically dihalo-substituted DIM was significantly more active than DIM, as inhibitors of estrogen-induced cell proliferation and tumor growth.[7]

To establish a possible relationship between the structure, activity and the mechanism of CYP induction, a series of 14 DIM analogs was synthesized and their CYP 1A1 induction activity was reported.[8] Because the mechanism of binding of DIM remains unclear, the present work was to elucidate the structural features involved in their mechanism of action by 3D-QSAR methods. DISCO[9] method was used to identify a common pharmacophore group of the molecules, then, CoMFA[10] analysis was used to demonstrate that the difference in the target property (CYP induction here) may be related to differences in the shape of the non-covalent fields surrounding the molecules.

Computational methods

A series of 14 DIM and DIM analogs was chosen. Their structure and biological data are summarized in Table 1. The activity data was expressed as percentage of the control increase in EROD activity (*A*), which was recognized as a good indicator of the CYP 450 1A1 activity.[11] Sybyl 6.7[12] was employed for all the calculations, which were performed on Silicon Graphics Octane 2 workstation.
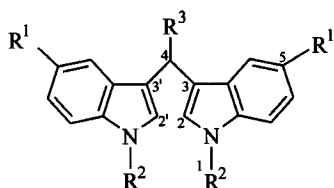
Fig. 1 Skeleton structure of diindolylmethane (DIM) compounds.

Table 1 Structures of diindolylmethane (DIM) and its analogs, and their ability to induce the catalytic activity of CYP1A1 (A) in H295R cells

	Substitution			Catalytic activity	
	R^1	R^2	R^3	A	lg A
DIM	H	H	H	710	2.85
B-DIM	Br	H	H	750	2.88
M-DIM	CH_3	H	H	625	2.80
MO-DIM	CH_3O	H	H	425	2.63
DIM-1	H	CH_3	p-$CH_3C_6H_4$	193	2.26
DIM-2	H	CH_3	p-C_6H_5	207	2.32
DIM-3	H	CH_3	p-$C_6H_5C_6H_4$	282	2.45
DIM-4	H	CH_3	p-$CF_3C_6H_4$	351	2.55
DIM-5	H	CH_3	p-$C_{10}H_7$	370	2.57
DIM-6	H	H	p-C_6H_5	153	2.18
DIM-7	H	H	p-OHC_6H_4	130	2.11
DIM-8	H	H	p-$C_6H_5C_6H_4$	162	2.21
DIM-9	H	H	p-$C_{10}H_7$	171	2.23
DIM-10	H	H	p-$CF_3C_6H_4$	144	2.16

Molecular modeling

The entire set of DIM analogs was built using the SKETCH option in Sybyl. Energy minimization was performed with Standard Tripos Molecular Mechanics force field, with a distance dependent dielectric function and a 0.21 kJ/mol energy gradient convergence. Partial atomic charges were calculated using the Gasteiger-Hükel protocol.

Conformational analysis and alignment rule

It is very important for CoMFA analysis to select a proper alignment rule. The conformational analysis was performed by MULTISEARCH method within the search routine in Sybyl. From every set of conformers generated, a suitable low energy conformation was selected for the DISCO (distance comparative) procedure of tripos to identify a common pharmacophore. According to the model of pharmacophore derived and the orientation of the hydrophobic site points identified on every conformer, the molecules were mutually aligned by root mean square (RMS) fitting of selected carbon atoms along the indole moieties.

CoMFA analysis

The CoMFA column value was performed with Sybyl

standard parameters. The steric and electrostatic fields energies (AM1 charge) were calculated using an sp^3 carbon probe atom with a charge of + 1 and a distance dependent dielectric constant at all intersection of a regularly spaced (0.2 nm) grid. Steric and electrostatic contributions were truncated at 126 kJ/mol. Partial Least Squares (PLS) applied was implemented in Sybyl.[10] Regression analysis was performed using cross-validation leave-one-out method. The optimal number of component to be used in the conventional analysis was defined as that which yielded the highest cross-validated q^2.

Results and discussion

Alignment and pharmacophore analysis

According to the RMS fitting of the selected carbons along the DIM common structure, the series of 14 compounds was properly aligned and represented in Fig. 2. The common reference compound used was DIM considered as a strong CYP 1A1 inducer.
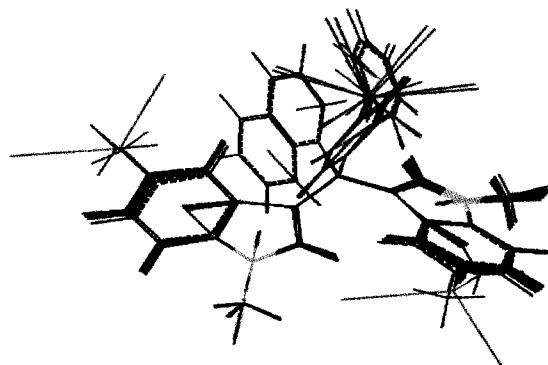

Fig. 2 Stereoview of the aligned molecular structures of 14 DIM compounds according to the common pharmacophore and atom-by-atom fit.

Because DIM compounds are considered as rigid analogs due to their rigid body, constituted by 2 indoles moieties, the DISCO pharmacophore model obtained emphasizes on the hydrophobic character of the molecules, by determining four hydrophobic site-points, as centroids for the four rings of the common structure of DIMs, and furnished hypothesis pharmacophore for superposition of the molecules. No further information was concluded about the binding site points of DIM to the TCDD receptor.

CoMFA and conformational analysis

CoMFA results are extremely sensitive to a number of factors such as alignment rules, overall orientation of aligned compounds, conformer selected, step size, the probe atom type, etc..[13] So we decided the alignment rules, step size and probe atom, then we applied q^2 guided conformer selection to select conformer. Two CoMFA models (A and B) were obtained. Model B included the lowest energy conformers. Model A included the large probability conformer. The model

parameters are showed in Table 2.

Table 2   Statistics parameters of PLS analysis

	Cross-validation		Conventional		
	q^2	Optimal component	r^2	SEE	F
CoMFA model A	0.827	5	0.988	0.044	103.53
CoMFA model B	0.226	4	0.975	0.055	75.55

The CoMFA model A obtained showed a high predictive ability with a cross-validation q^2 value of 0.827. The conventional correlation coefficient r^2 value was 0.988, $F = 103.53$ and standard error estimate (SEE) was 0.044. While model B showed poor predictive ability whose q^2 is only 0.226, so it is testified that how to select conformer is very important to CoMFA model.

From those results of Table 2, it appears to us that the DISCO model derived had guided us to a correct alignment rule which is aligned according to pharmacophore. Different molecule used as reference compound had little effect on the CoMFA result. Furthermore, the indoles moieties with the apparent rigidity show that rotating around the central carbon is possible, as none of the low-energy conformations used in the alignment set is planar or almost planar. Nevertheless, they all are biplanar with 2 dihedral angle values of 120° and 4° for C2-C3-$C_{central}$-C3′ and C2′-C3′-$C_{central}$-C3 torsion angles respectively. They differ from known CYP1A1 inducers, which have in common a planar or an energetically coplanar system, such as ICZ, TCDD or benzophenones.[14] Thus, this flexibility of the structure may reduce the receptor affinity of DIM compounds.

To check if a planar conformer of DIM can be achieved and to measure the rotational energy barrier of it, the torsion angles C2-C3-C4-C3′ and C2′-C3′-C4-C3 were modified to 0° and the conformer energy was minimized again with Tripos force field. The planar conformer was obtained, whose energy was lower by 29.4 kJ/mol than the original conformer. In conclusion, this planar conformer characterizing specific CYP 1A1 inducers with a barrier of energy of only 29.4 kJ/mol may be achieved by DIM *in vivo* but not *in vitro*.

To evaluate the predicting ability of the CoMFA model A, the activity of a compound set was predicted. The experimental and the predicted activity values and their residual are presented in Table 3 and Fig. 3.

The values on Table 3 indicate that for the model CoM-FA, the residual values are all smaller than 2%. The plot in Fig. 2 illustrates the small difference between the actual and the predicted data of our model. So that all the points are close to each other, in both sides of the diagonal line, demonstrating that the resulted CoMFA model has a fair predicting ability.

CoMFA coefficient contour maps

The 3D contour maps were generated to represent the

Table 3   Experimental activities (Ea) and predicted activities (Pa) by the CoMFA model A

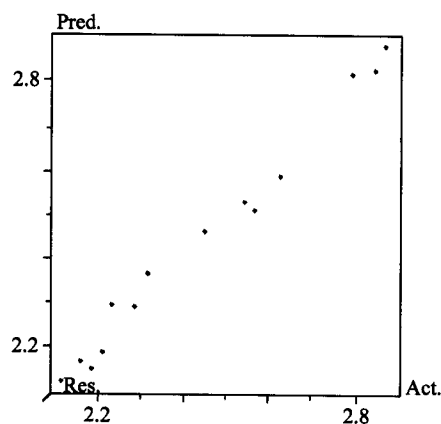| Compound	lg A		
	Ea	Pa	Δ Value
DIM	2.85	2.834	− 0.02
B-DIM	2.88	2.889	0.01
M-DIM	2.80	2.825	0.03
MO-DIM	2.63	2.591	− 0.04
DIM-1	2.26	2.291	0.01
DIM-2	2.32	2.365	0.05
DIM-3	2.45	2.463	0.01
DIM-4	2.55	2.532	− 0.01
DIM-5	2.57	2.513	− 0.05
DIM-6	2.18	2.149	− 0.04
DIM-7	2.11	2.119	0.00
DIM-8	2.21	2.186	− 0.02
DIM-9	2.23	2.294	0.06
DIM-10	2.16	2.164	0.01

Fig. 3   Plot of actual versus predicted data from the CoMFA model A.

QSAR result produced by CoMFA. The contributions of the steric and the electrostatic field to the activity were 63.2% and 36.8%, respectively by PLS analysis. Figs. 4 and 5 show a stereocolors views of 3D steric and electrostatic map.
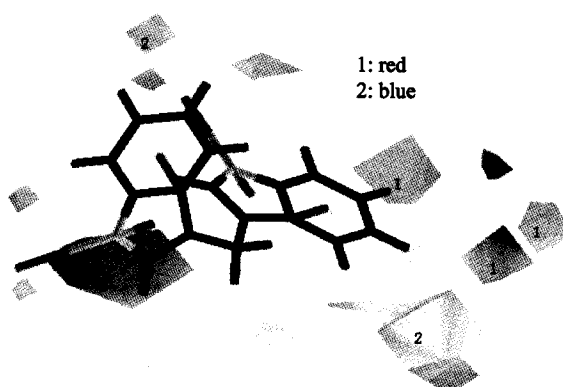

Fig. 4   CoMFA electrostatic contour map. (1) Negative potential favorable; (2) positive potential favorable.
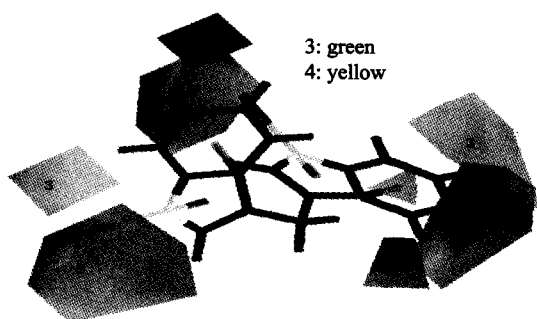
3: green
4: yellow

Fig. 5 CoMFA steric contour map. (3) Sterically favorable; (4) sterically unfavorable.

The electrostatic fields are in red and blue. The yellow contours indicate the regions of negative steric potential while the green contours indicate the regions of positive steric potential. Similarly, the red contours mark the regions of negative electrostatic potential and the blue contours indicate the regions of positive electrostatic potential. To aid in visualization, the potent DIM is displayed in each of the maps.

Of particular interesting, we note that the substitution on the central carbon, where the yellow polyhedron is displayed, decreases the EROD activity (see Fig. 1, Table 1). This is likely due to the bulky groups on the central carbon, which would prevent the molecule from achieving the coplanar structure required for interaction with the Ah receptor. In contrast, symmetrical substitution on the N position in Fig. 1 with bulky groups, such as alkyl or aryl, increased significantly the catalytic activity of those compounds, certainly due to the lipophilic character of the tertiary amines of DIMs, and it is known that CYP1A1 inducers are highly lipophilic.[15] If the substitution of R^1 is halogen, Cl, Br, or alkyl, etc., because they are electron donors, it will stabilize the indole ring and enhance the catalysis activity.

Based on those results, and according to the CoMFA model A, a group of newly designed compounds is cited in Table 4. Substitution was done symmetrically on the R^4, R^5 and R^6 positions, separately or not, with different bulky groups. 12 new designed compounds (Fig. 6) exhibited a high predicted activity as well, compared to DIM candidate activity value (2.835) expressed in Table 3.

Conclusion

We have performed a first 3D-QSAR study on 14 anticarcinogenic/antitumoric DIMs analogs compounds by means of the CoMFA analysis. We used the DISCO method within the SYBYL software to determine the common pharmacophore group of the structures to align them. The CoMFA model derived showed high predictive ability, as the contribution of the steric field to the activity was 63,8%, and the green polyhedron in the steric map surrounded the azote atoms of the common structure of DIM compounds. This means that more bulky and hydrophobic substituants are beneficial to the activity. According to those structural modifications, we designed some new compounds, which provide us some ideas for syn-

thesis of further DIMs analogs not reported yet, which may exhibit catalytic, antiestrogenic-antitumoric activity.

Table 4 New designed compounds expressing higher predictive activity (Pa)

No.	R^4	R^5	R^6	Pa
1	5-Br	C_6H_5	H	3.02
2	5-Br	$CH(CH_3)_2$	H	3.08
3	5-Me	$CH(CH_3)_2$	H	3.07
4	5-Me	C_2H_5OH	H	3.07
5	5-Br	$COCH_3$	H	3.00
6	H	$CH(CH_3)_2$	H	3.00
7	H	C_2H_5OH	H	3.02
8	H	α-furyl	H	2.93
9	5-$CONH_2$	H	H	2.90
10	5-$COCH_3$	H	H	2.91
11	H	H	OCH_3	3.06
12	H	H	COC_2H_5	2.88
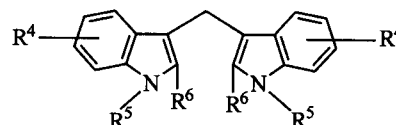
Fig. 6 Skeleton structure of new designed compounds.

Acknowledgement

References

1 Sondik, E. *J. Cancer* **1994**, *74*, 995.

2 Jordan, V. C. *Breast Cancer Res. Treat.* **1994**, *31*, 41.

3 De Kruif, C. A.; Marsman, J. W.; Venekamp, J. C.; Falke, H. E.; Noordhoeek, J.; Blaauber, B. *J. Chem. Biol. Interact.* **1991**, *80*, 303.

4 Jellinck, P. H.; Forkert, P. G.; Riddick, D. S.; Okey, A. B.; Michnovich, J. J.; Bradlow, H. L. *Biochem. Pharmacol.* **1993**, *45*, 1129.

5 Chen, I.; McDougal, A.; Wang, F.; Safe, S. *Carcinogenesis* **1998**, *19*, 1631.

6 McDougal, A.; Gupta, M. S.; Morrow, D.; Ramamoorthy, K.; Lee, J. E.; Safe, S. *Breast Cancer Res. Treat.* **2001**, *66*, 147.

7 McDougal, A.; Gupta, M. S.; Morrow, D.; Ramamoorthy, K.; Sun, G.; Safe, S. *Cancer Lett.* **2000**, *151*, 169.

8 Sanderson, J. T.; Slobbe, L.; Lansbergen, W. A.; Safe, S.; Van Den Berg, M. *Toxicol. Sci.* **2001**, *61*, 40.

9 Martin, Y. C.; Bures, M. G.; Danaher, E. A.; DeLazzer, J.; Lico, I.; Pavlik, P. A. *J. Comput.-Aided Mol. Des.* **1993**, *7*, 83.

10 Cramer III, R. D.; Patterson, D. E.; Bunce, J. D. *J. Am.*

Chem. Soc. **1988**, *110*, 5959.

11   Cho, S. J.; Tropsha, A. *J. Med. Chem*. **1995**, *38*, 1060.

12   *Sybyl* [*computer program*]. Version 6.7, Tripos Associates, St Louis (MO), **1999**.

13   Tropsha, A.; Cho, S. J. in *3D QSAR in Drug Design*, Vol. 3,

Eds.: Kubinyi, H.; Folkers, G.; Martin, Y. C., KLUWER/ ESCOM, Dordrecht, **1998**, p. 57.

14   Gillner, M.; Bergman, J.; Cambillau, C.; Fernstrom, B.; Gustafsson, J. A. *Mol. Pharmacol*. **1985**, *28*, 357.

15   Sandoz, A. *Arch. Biochem. Biophys*. **2000**, *373*, 275.

(E0204244   ZHAO, X. J.; DONG, H. Z.)